

SCIENTIFIC REPORTS



OPEN

Smelting reduction and kinetics analysis of magnetic iron in copper slag using waste cooking oil

Bo Li¹, Xubin Wang², Hua Wang¹, Yonggang Wei¹ & Jianhang Hu²

To improve the recovery of copper, the viscosity of copper molten slag is decreased by the reduction of magnetic iron, which, in turn, accelerates the settling and separation of copper droplets from the slag. A new technology is proposed in which waste cooking oil is used as a reductant to reduce magnetic iron in the copper smelting slag and consequently reduce carbon emissions in the copper smelting process. A kinetic model of the reduction of magnetic iron in copper slag by waste cooking oil was built using experimental data, and the accuracy of the model was verified. The results indicated that the magnetic iron content in the copper slag decreased with increasing reduction time and an increase in temperature more efficiently reduced magnetic iron in the copper slag. The magnetic iron in the copper slag gradually transformed to fayalite, and the viscosity of the copper molten slag decreased as the magnetic iron content decreased during the reduction process. The reduction of magnetic iron in the copper molten slag using waste cooking oil was a first-order reaction, and the rate-limiting step was the mass transfer of Fe_3O_4 through the liquid boundary layer.

Energy is indispensable to human beings, and the development of human society is closely related to the development and utilization of energy. Fossil fuels, including coal, oil and natural gas, have long been the primary energy source and main driving force behind industrial development and social progress. However, nonrenewable fossil fuels are a finite resource, and finding efficient, large-scale alternative energy sources is an urgent matter. The annual consumption of edible oils in China has reached tens of millions of tons. According to a waste cooking oil market analysis, the food and beverage industry generates approximately 2000 million tons of waste cooking oil in China every year, only 8% of which is used for industrial production. Finding additional uses for waste cooking oil could result in both energy savings and emission reductions. Several groups have investigated the use of waste cooking oil as a resource for biodiesel production. Li M.¹ studied biodiesel production from waste cooking oil using a heterogeneous catalyst from pyrolysed rice husks. In the presence of the as-prepared catalyst, the free fatty acid conversion reached 98.17% after 3 h, and the fatty acid methyl ester yield reached 87.57% after 15 h. The production of biodiesel from waste palm cooking oil using acidic ionic liquid as a catalyst was investigated by Ullah Z.² The highest biodiesel yield was obtained with 5 wt.% BMIMHSO₄, a methanol:oil ratio of 15:1, a 60 min reaction time, a temperature of 160 °C, and an agitation speed of 600 rpm, which reduced the waste cooking oil acid value to below 1.0 mg KOH/g. The final yield was 95.65 wt.%. Various studies have shown that biodiesel made from waste cooking oil can be used in diesel engines. Can Ö.³ studied a mixture of biodiesel fuels produced from two types of waste cooking oils blended with 5% and 10% diesel fuel. The results showed that an addition of 5% and 10% biodiesel fuel resulted in a slight increase in the break specific fuel consumption (up to 4%) and a reduction in break thermal efficiency (up to 2.8%). The biodiesel additions increased the NO_x emissions by up to 8.7% and decreased the smoke and total hydrocarbon emissions at all engine loads. Elshaib A.A.⁴ studied the combustion characteristics, performance and exhaust emissions of a direct injection diesel engine fuelled by a diesel/biodiesel blend from waste cooking oil up to B100. The soot peak volume fraction was reduced by 15.2%, whereas the CO and HC concentrations decreased by 20 and 28.5%, respectively. The physical and chemical delay periods decreased by 1.2 and 15.8%, respectively, which resulted in an engine noise reduction of 6.5%.

Large amounts of copper slag containing significant amounts of valuable metals can be produced in the copper pyrometallurgy process. In the long term, copper slag will become a wasted resource, occupy considerable land

¹State Key Laboratory of Complex Nonferrous Metal Resources Clean Utilization, Kunming University of Science and Technology, Kunming, 650093, China. ²Faculty of Metallurgy and Energy Engineering, Kunming University of Science and Technology, Kunming, 650093, China. Correspondence and requests for materials should be addressed to B.L. (email: libokmust@163.com)

Element	C	H	O	N	S
Content (wt.%)	77.81	12.33	8.93	0.86	0.07

Table 1. Elemental composition of waste cooking oil.

Element	SiO ₂	Fe ₃ O ₄	CaO	Al ₂ O ₃	MgO	S	Cu
Content (wt.%)	34.36	17.80	6.44	5.29	4.38	0.85	0.58

Table 2. Chemical composition of copper slag.

and cause serious environmental pollution; thus, methods to further process copper slag must be developed⁵. Both chemical and physical processes contribute to copper loss in slag inclusions; however, the main reason for the loss is that strong oxidation during copper smelting can increase the magnetic iron content in the slag, which increases the viscosity and surface tension of the copper slag, causing copper slag separation to deteriorate. To reduce the copper content in the slag and improve the copper recovery, the copper slag is diluted to reduce the magnetic iron content in the slag, increase the slag mobility, and promote the settling of matte droplets⁶.

Because the copper smelting slag contains large amounts of magnetic iron, the modification of copper slag involves the reduction of iron oxides in the slag. In recent years, several studies investigating the reduction of magnetic iron in copper slag have been performed. Michal E.J.⁷ studied the effect of the CO₂/CO ratio on the Fe³⁺/Fe²⁺ ratio by carbon in the Fe₃O₄ reduction process. The results showed that the magnetic iron phase increased with an increase in CO₂ partial pressure in a reduction atmosphere and that the key factor for selective reduction by a carbonaceous reductant was control of the reducing atmosphere. Matousek J.M.⁸ summarized the effect of the reduction potential and Fe/SiO₂ ratio on the carbon reduction process of molten copper slag at 1250 K and showed that the transformation of Fe³⁺ to Fe²⁺ in the slag requires a lower oxygen potential. The lower oxygen potential may generate metallic iron due to excessive reduction; thus, the oxygen potential should be controlled in the range of 10⁻⁹–10⁻¹⁰. Additionally, increasing the SiO₂ content is more conducive to the reduction of Fe₃O₄. The carbon-reduced smelting of copper slag under nitrogen gas with stirring was studied by Zhang L.N.⁹. The results showed that the Fe₃O₄ content in the slag gradually decreased and that the main phase in the residue after the reaction included the residual magnetic iron olivine and calcium silicon solid solution. The thermodynamics and kinetics of the CH₄ reduction of molten copper slag was studied by Riveros G. *et al.*¹⁰. The results showed that the reduction of Fe₃O₄ by CH₄ was a first-order reaction and that the apparent activation energy of Fe₃O₄ reduction by CH₄ was 62 kJ/mol, which is much lower than that when CO is used as a reducing agent¹¹. Zhan H.W.¹² studied a method of cleaning copper slag using an electric field and a slag reduction modification with mixed CH₂ gas. These results showed that in the molten slag reduction process, the reduction rate increased with an increase in H₂ content in the mixed gas and that the viscosity of the molten slag efficiently decreased; the phase transformation of copper oxide in the reduction process was as follows: CuFe₂O₄ → Cu₂O → CuO. The interfacial interaction between the copper matte particles and the molten slag presented an opportunity to use the electrocapillary phenomenon in the slag-cleaning process. The presence of certain electric fields accelerated the migration of copper drops from the anode to the cathode and improved the copper slag cleaning. The settling rate with an electric field of 1.5 V·cm⁻¹ was two or three times higher than the natural settling with only gravity.

Several traditional reducing agents, such as pulverized coal, coke, diesel and natural gas, can be used to reduce magnetic iron in copper slag in an electric furnace with the blowing and stirring method. The main elements of waste cooking oil are C, H, and O; thus, the chemical composition of waste cooking oil, which is a green resource, is notably similar to that of petroleum diesel. It is highly significant that a waste resource, such as waste cooking oil, can be used in a copper slag depletion process thereby reducing carbon emissions.

Test Materials and Methods

Test materials. The waste cooking oil used in this study was obtained from the waste oil and fats from the food and beverage industry in Kunming. The chemical compositions are shown in Table 1. The primary elements of the waste cooking oil were C, H, and O with a small quantity of N and S. C and H accounted for 90% of the total waste cooking oil, and the O content was also notable. In the high-temperature pyrolysis process, high temperature was more beneficial to the gasification and generation of gas-phase products. The copper slag used in this study was the electric furnace slag from the Yunnan copper factory; its chemical composition is shown in Table 2.

Test apparatus and method. The apparatus for reducing magnetic iron using waste cooking oil is shown in Fig. 1. The main component of the equipment is an electric tube furnace. A crucible with copper slag was placed in the furnace tube, and the top of the furnace tube was sealed using a stainless steel flange seal. First, argon gas was bubbled into the furnace tube to remove any remaining air in the device before the experiment. Next, the furnace temperature was increased to the experimental temperature and maintained for 40 min. After the waste cooking oil was preheated to 50 °C, it was blown into the copper slag sample using a peristaltic pump with argon as the carrier gas. The oil flow was 1 mL/min, and the argon flow was 3 L/min during the experiment. To sufficiently reduce and deposit copper matte droplets in the slag, the temperature was maintained for 30 min after the end of the experiment. Highly pure argon gas at a flow rate of 600 mL/min was used as a protective gas in the cooling process.

The elemental composition of C, H and N in the waste cooking oil was determined using a Perkin Elmer 2400 Series II element analyser, the S content was determined with a TS-2000 sulfur content analyser, and the O content was obtained in a difference calculation. X-ray diffraction techniques were used to measure the phase changes using

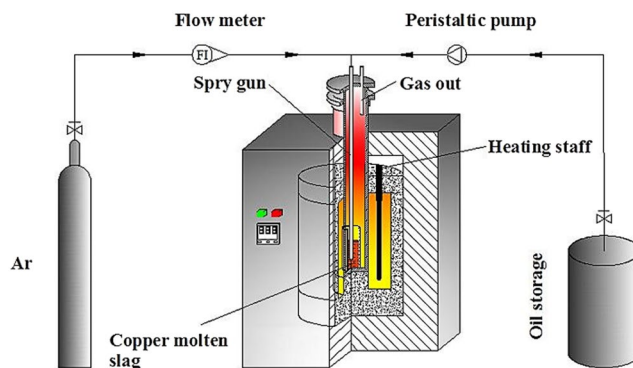


Figure 1. The apparatus of magnetic iron reduction by waste cooking oil.

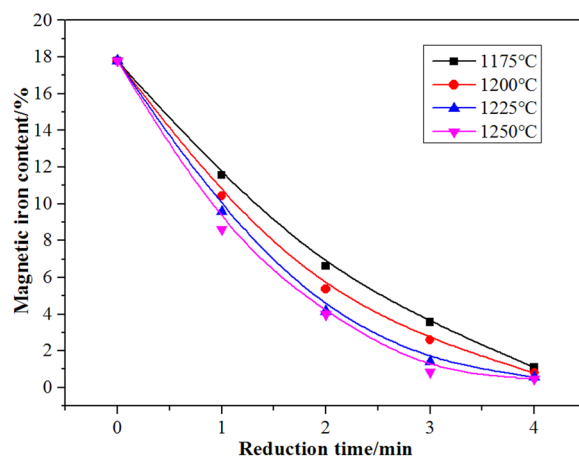


Figure 2. The change of content of magnetic iron with reduction time at different temperatures.

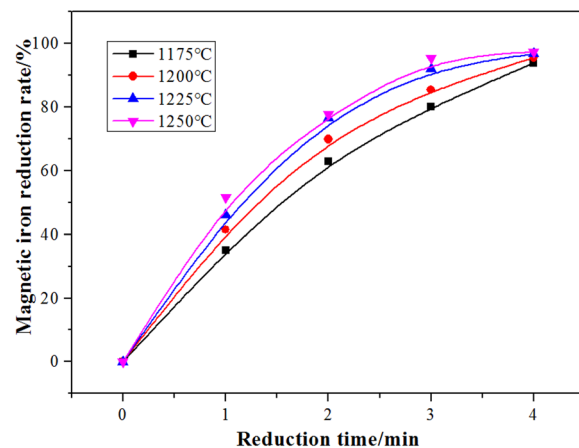


Figure 3. The change of reduction rate of magnetic iron with reduction time at different temperatures.

a Cu-K α radiation source (35 kV, 20 mA) to obtain data at a scanning rate of 8°/min over the angular range of 10° to 90°. A scanning electron microscopy analysis of the concentrates was performed using a HITACHI-S3400N SEM with a BSE resolution of 4.0 nm (30 kV). An energy dispersive spectroscopy analysis was performed using EDAX. The magnetic iron content of the experimental product was analysed using a Satmagan135 magnetic analyser.

Discussion

Change in the magnetic iron content in the copper slag during the reduction process. Figure 2 and Fig. 3 show the changes in the content and reduction rate of magnetic iron with respect to the reduction reaction time at different temperatures. When the reduction time reached 4 min, the magnetic iron content in the slag

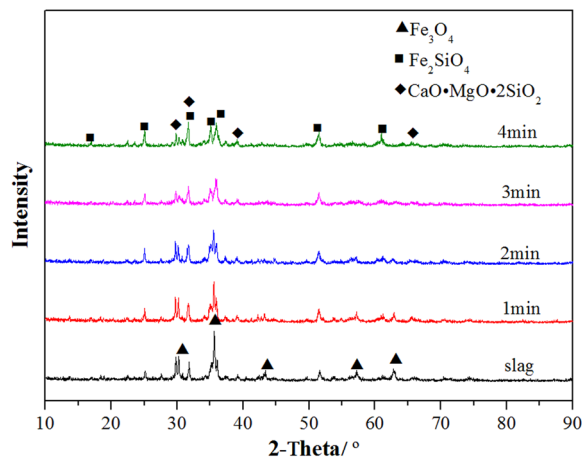


Figure 4. XRD patterns of copper slag for different times (1175 °C).

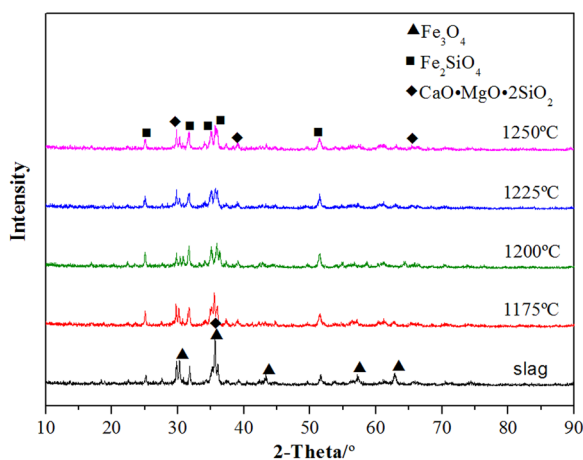


Figure 5. XRD patterns of copper slag for different temperatures (2 min).

decreased to below 2% and the reduction rate of magnetic iron was greater than 90%. These results showed that the magnetic iron in the copper slag was significantly reduced using waste oil. As the temperature increased, the reduction rate of the magnetic iron in the copper slag slightly increased. Because the viscosity of the copper slag decreased with increasing temperature, the dynamic conditions of reduction were improved.

Analysis of the phase and viscosity of the copper slag in the reduction process. The XRD patterns of the copper slag that was reduced using waste oil at 1175 °C for different reduction times are shown in Fig. 4. Magnetic iron (Fe_3O_4), the main phase in electric furnace slag, was transformed into fayalite (Fe_2SiO_4) and a silicate solid solution, which included calcium magnesium oxide. As the reduction time increased, the peak intensity of the magnetic iron in the copper slag gradually decreased and the peak intensity of fayalite gradually increased. The results show that the magnetic iron in the copper slag is transformed into fayalite in the reduction process. The magnetic iron in the slag is reduced to FeO, which generates fayalite and SiO_2 .

Figure 5 shows the XRD patterns of the copper slag reduced at different temperatures for 2 min. Compared with the original slag, the peak intensities of the magnetic iron in the reduced copper slag are much weaker than those under other conditions. As the temperature increased, the peak intensity of the magnetic iron in the copper slag gradually decreased, and the peak intensity of fayalite gradually increased. Compared with the reduction time, the temperature has a smaller effect on the phase of the copper slag.

The SEM patterns of the copper slag that was reduced at 1175 °C for various durations are shown in Fig. 6. With an increase in reduction time, the magnetic iron regions decreased in intensity, and the fayalite regions gradually increased. Thus, the magnetic iron phase was converted to fayalite with the reduction of the copper slag.

The waste cooking oil decreased the slag viscosity by reducing the magnetic iron content in the copper slag. Decreasing the slag viscosity can improve the kinetics of the separation of copper slag droplets. The viscosity of the sample was determined at a reduction temperature of 1175 °C for different reduction times. The viscosity curves of the samples at different temperatures are shown in Fig. 7. The viscosity of the copper slag decreases with an increase in reduction time. Generally, the copper slag viscosity is less than 0.5 Pa·s, and the copper slag can be considered to have good liquidity; later, the viscosity increases to greater than 1 Pa·s, which is considered

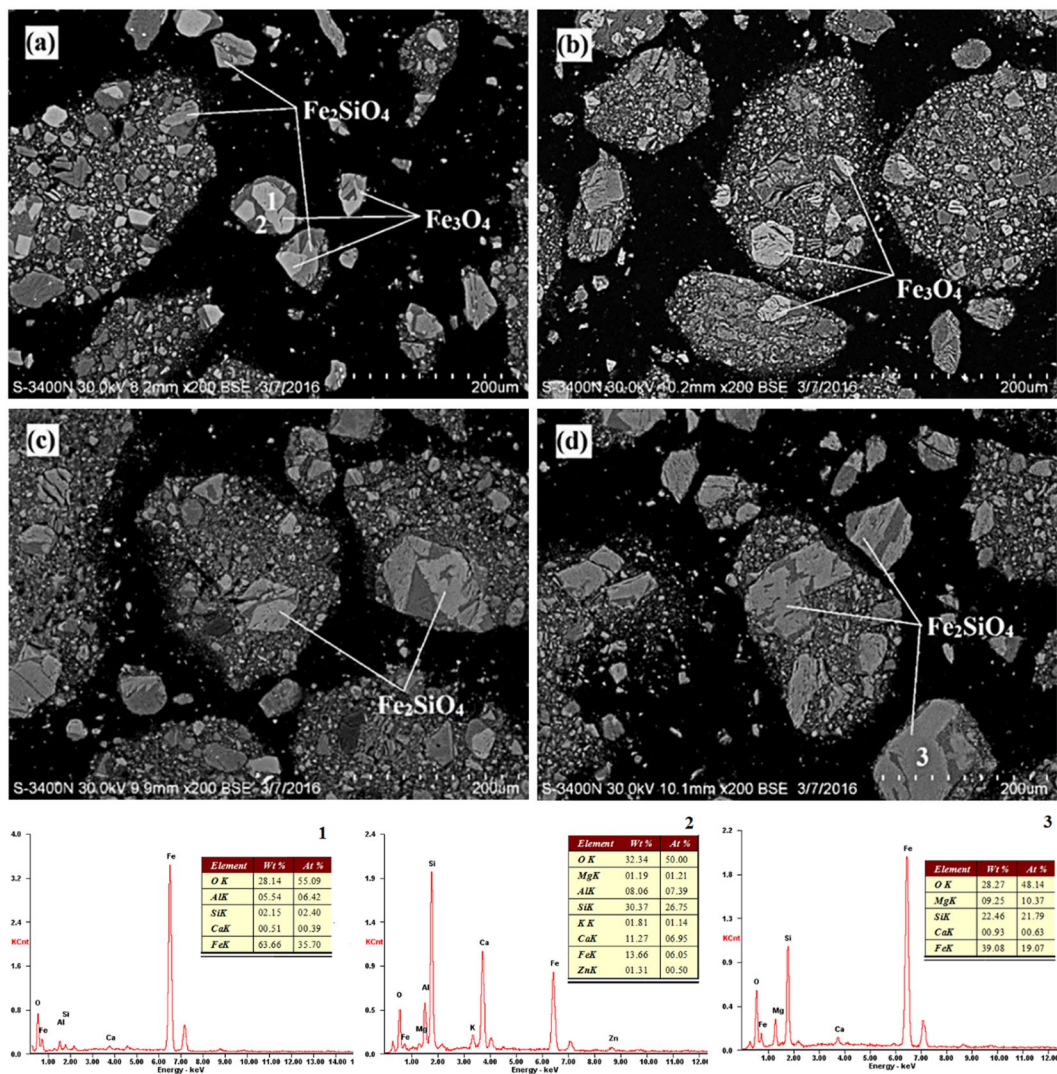


Figure 6. The SEM patterns of copper slag for different reduction times (1175 °C): (a) 1 min, (b) 2 min, (c) 3 min, (d) 4 min.

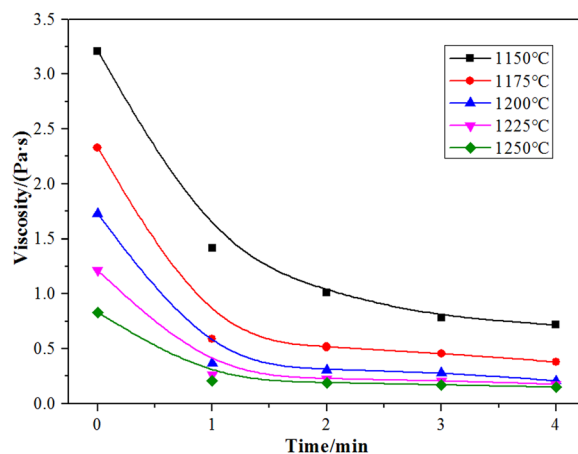


Figure 7. The relationship between the viscosity of copper slag and the reduction time.

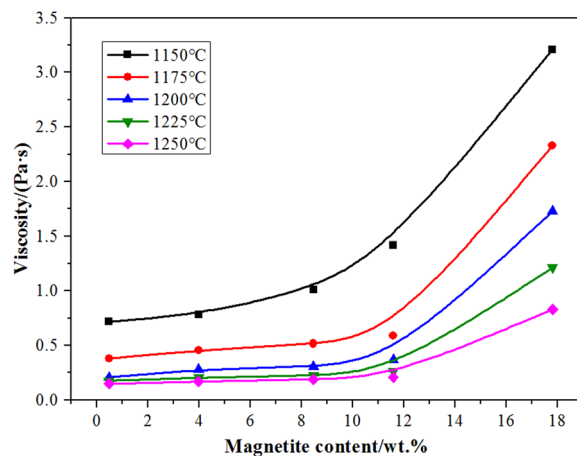


Figure 8. The relationship between the variety of Fe_3O_4 content in slag and the viscosity of copper slag.

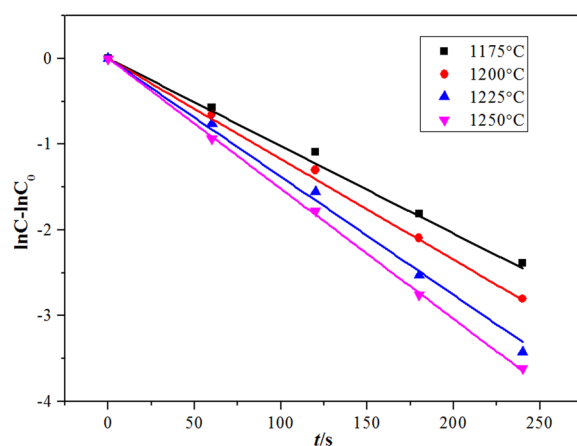


Figure 9. The relationship between the concentration of Fe_3O_4 in copper slag and reaction time ($n = 1$).

poor liquidity¹³. When the reduction time is 3 min, the copper slag viscosity decreases to 1 Pa.s. The relationship between the magnetic iron content and the viscosity of the copper slag at different reduction temperatures is shown in Fig. 8. When the magnetic iron content in the copper slag is below 10%, the slag viscosity does not change significantly. However, when the magnetic iron content is above 10%, the slag viscosity increases sharply with increasing magnetic iron content.

Kinetics analysis of the reduction of magnetic iron. The relationship between the magnetic iron concentration in the copper slag and the reaction time of the copper slag reduction by waste cooking oil is shown in Fig. 9. Because a linear correlation between the magnetic iron concentration and the reaction time is better for the reaction order ($n = 1$), the reduction of magnetic iron in the copper slag is a first-order reaction¹⁴. According to gas-liquid reaction kinetics, when the logarithm of the concentration of the diffusion components in the liquid phase is linearly related to the reaction time, the gas-liquid reaction is controlled by the liquid phase mass transfer. Thus, the reduction of magnetic iron in the copper slag by waste cooking oil is controlled by liquid phase mass transfer^{15,16}. Figure 10 shows the relationship between $\ln K$ and $1/T$ at different temperatures. Because the linearity is notably good, the apparent activation energy and frequency factor, which were obtained from the intercept and slope of a fitted straight line, are shown in Table 3. The apparent activation energy is 99.3 kJ/mol, and the pre-exponential factor is 39.2.

The pyrolysis of waste cooking oil rapidly forms small gaseous molecules and coke at high temperature; thus, the reduction of magnetic iron in copper slag is a gas-liquid-solid phase reaction. Following the double-film theory, the reaction model of magnetic iron reduction in copper slag by waste cooking oil is shown in Fig. 11.

When bubbles come into contact with the slag, a stable phase interface is formed on both layers of the vapour film and the layer of the liquid film. The resistance to mass transfer mainly occurs in the two-layer films. The reducing gas diffuses from the body of the gas phase to the gas-liquid phase interface in the bubbles. Fe_3O_4 diffuses from the body of the liquid slag to the gas-liquid phase interface. The reaction generates reductants, such as FeO , CO_2 , and H_2O , at the gas-liquid phase interface, and FeO diffuses into the slag body. The gas products diffuse into the body of the gas phase, which may continue to react with coke to generate CO and H_2 ¹⁷⁻¹⁹.

The reduction of magnetic iron by waste cooking oil is controlled by the liquid phase:

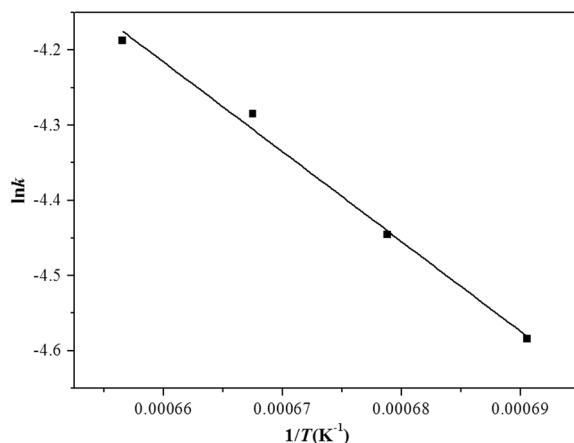


Figure 10. The relationship between $\ln k$ and $1/T$.

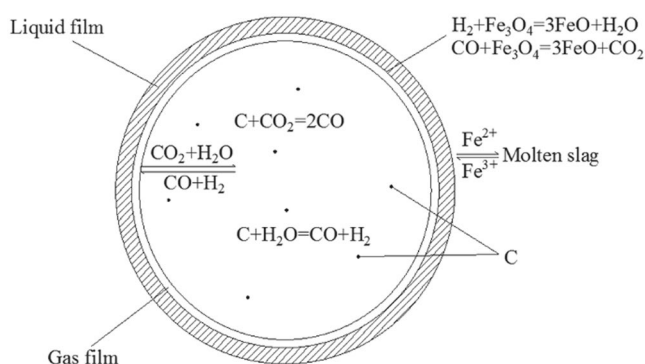


Figure 11. The reaction model of magnetic iron in the reduction process of copper slag by waste cooking oil.

$T/^{\circ}\text{C}$	k/s^{-1}	n	$E/\text{kJ}\cdot\text{mol}^{-1}$	A/s^{-1}
1175	0.01021	1	99.3	39.2
1200	0.01173			
1225	0.01378			
1250	0.01519			

Table 3. Kinetic parameters of magnetic iron in the reduction of copper slag.

$$k = k_{\text{Fe}_3\text{O}_4} \tag{1}$$

The mass transfer flux of Fe_3O_4 through a liquid membrane²⁰ can be represented as follows:

$$J_{\text{Fe}_3\text{O}_4} = k_{\text{Fe}_3\text{O}_4} (C_{\text{Fe}_3\text{O}_4} - C_{\text{Fe}_3\text{O}_4}^*) \tag{2}$$

where $J_{\text{Fe}_3\text{O}_4}$ is the mass transfer flux, $\text{mol}/(\text{m}^2\cdot\text{s})$; $k_{\text{Fe}_3\text{O}_4}$ is the Fe_3O_4 mass transfer coefficient, m/s ; $C_{\text{Fe}_3\text{O}_4}$ is the Fe_3O_4 concentration in the slag body, mol/m^3 , and $C_{\text{Fe}_3\text{O}_4}^*$ is the Fe_3O_4 concentration at the gas-liquid interface, mol/m^3 .

According to the film-penetration theory²¹, the mass transfer coefficient can be expressed as:

$$k_{\text{Fe}_3\text{O}_4} = 2 \sqrt{\frac{D_{\text{Fe}_3\text{O}_4}}{\pi t_c}} \tag{3}$$

where $D_{\text{Fe}_3\text{O}_4}$ is the diffusion coefficient of Fe_3O_4 in the liquid film, m^2/s , and t_c is the mass transfer time. From this, the following formula can be obtained:

Temperature $T/^{\circ}\text{C}$	Density $\rho_l /$ $\text{kg}\cdot\text{m}^{-3}$	Viscosity $\mu_l /$ $\text{Pa}\cdot\text{s}$	surface tension σ $/10^{-3}\text{N}\cdot\text{m}^{-1}$
1175	3566	2.33	575.28
1200	3438	1.73	605.45
1225	3351	1.21	635.62
1250	3306	0.83	665.78

Table 4. Physical parameters of slag under different temperatures.

Temperature $T/^{\circ}\text{C}$	H_2 productivity / $\text{mL}\cdot\text{min}^{-1}$	CO productivity / $\text{mL}\cdot\text{min}^{-1}$	Total productivity $/\text{mL}\cdot\text{min}^{-1}$	Coke productivity $/\text{g}\cdot\text{min}^{-1}$
1175	776	97	873	0.51
1200	819	105	924	0.52
1225	838	112	951	0.53
1250	858	120	978	0.54

Table 5. Pyrolysis of waste oil in different temperature.

Temperature $T/^{\circ}\text{C}$	Density $\rho_b /$ $\text{kg}\cdot\text{m}^{-3}$	Diameter d_e / m	Residence time t_e / s	Diffusion coefficient $D_{\text{Fe}_3\text{O}_4}$ $/\text{m}^2\cdot\text{s}^{-1}$	Floating velocity $u_b /$ $\text{m}\cdot\text{s}^{-1}$
1175	0.287	8.40×10^{-3}	0.113	9.16×10^{-6}	0.074
1200	0.280	8.71×10^{-3}	0.086	9.56×10^{-6}	0.100
1225	0.274	8.87×10^{-3}	0.066	9.51×10^{-6}	0.135
1250	0.268	9.04×10^{-3}	0.051	9.36×10^{-6}	0.177

Table 6. Bubble characteristic parameters at different temperatures.

Temperature $T/^{\circ}\text{C}$	Re	Sc	Sh
1175	0.95	71.3	9.36
1200	1.73	52.6	10.69
1225	3.32	38.0	12.85
1250	6.37	26.8	14.67

Table 7. Bubble motion criterion at different temperatures.

$$t_c = d_e / u_b \quad (4)$$

when the gas flow at the nozzle exit is small, the size of the bubble is determined by the balance between the buoyancy and the surface tension²¹:

$$\frac{\pi}{6} d_e^3 (\rho_l - \rho_b) g = \pi d_0 \sigma \quad (5)$$

where d_e is the bubble diameter, m; ρ_l is the slag density, kg/m^3 ; ρ_b is the bubble density, kg/m^3 ; σ is the surface tension of the slag, N/m ; and d_0 is the nozzle inner diameter, m.

The floatation speed of a bubble in the slag is calculated using the Stokes formula¹²:

$$u_b = \frac{d_e^2}{12\mu_l} (\rho_l - \rho_g) \quad (6)$$

where μ_l is the slag viscosity, $\text{Pa}\cdot\text{s}$.

The mass transfer coefficient between the slag and the bubble is related to the bubble movement and the diffusion phase. Based on experimental data, the semi-empirical and semi-theoretical formulae were fitted and the criterion numbers are as follows^{22, 23}:

Reynolds number:

$$\text{Re} = \frac{\rho_l u_b d_e}{\mu_l} \quad (7)$$

Sherwood standard:

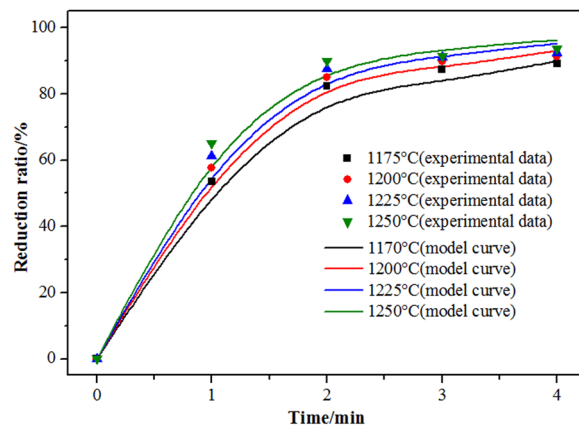


Figure 12. Comparison of numerical and experimental data (2 mL/min).

$$Sh = \frac{k_d d_e}{D} \quad (8)$$

Schmidt standard:

$$Sc = \frac{\mu_l}{\rho_l D} \quad (9)$$

The mass transfer coefficient between the bubbles and the slag can be expressed as:

$$Sh = m Re^n Sc^l \quad (10)$$

The parameters related to the kinetics analysis at different temperatures are shown in Tables 4–7. A nonlinear fit of the multi-variables and multi-parameters provides the undetermined parameters²⁴.

$$Sh = 4.13 \times 10^{-3} \cdot Re^{1.18} \cdot Sc^{1.82} \quad (11)$$

The reduction rate of magnetic iron can be expressed as:

$$R = \left(1 - e^{-4.13 \times 10^{-3} \cdot \frac{u_b^{1.18} \mu_l^{0.64} d_e^{0.18}}{\rho_l^{0.64} D_{Fe_3O_4}^{0.82}} t} \right) \times 100\% \quad (12)$$

To validate the accuracy of the model, the flow of waste cooking oil in the experimental process was set at 2 mL/min. The experimental data for the reduction rate of magnetic iron at different temperatures and the calculated data based on the above model are shown in Fig. 12. The results show that the experimental data are consistent with the calculated results.

Conclusions

Waste cooking oil is a green resource. It is highly significant that waste cooking oil is used in a copper slag depletion process to achieve waste resource utilization and reduce carbon emissions. In this study, electric furnace copper slag was found to be composed of magnetic iron (Fe_3O_4), fayalite (Fe_2SiO_4), calcium magnesium oxide, and a silicate solid solution. The magnetic iron content in the copper slag decreased with an increase in reduction time at different temperatures. With a reduction time of 4 min, the magnetic iron content in the copper slag was reduced to less than 2%, and the reduction efficiency of magnetic iron exceeded 90%.

When the magnetic iron content in the copper slag was below 10%, the slag viscosity did not noticeably change. However, when the magnetic iron content was above 10%, the slag viscosity increased sharply with increasing magnetic iron content.

The reduction of magnetic iron in the copper slag was shown to be a first-order reaction, and the apparent activation energy was 99.3 kJ/mol. The reduction of magnetic iron was controlled by liquid phase mass transfer, and the reduction rate of magnetic iron can be expressed as:

$$R = \left(1 - e^{-4.13 \times 10^{-3} \cdot \frac{u_b^{1.18} \mu_l^{0.64} d_e^{0.18}}{\rho_l^{0.64} D_{Fe_3O_4}^{0.82}} t} \right) \times 100\%$$

References

- Li, M. *et al.* Biodiesel production from waste cooking oil using a heterogeneous catalyst from pyrolyzed rice husk. *Bioresour. Technol.* **154**, 345–348 (2014).
- Ullah, Z., Bustam, M. A. & Man, Z. Biodiesel production from waste cooking oil by acidic ionic liquid as a catalyst. *Renew. Energy*. **77**, 521–526 (2015).
- Can, Ö. Combustion characteristics, performance and exhaust emissions of a diesel engine fueled with a waste cooking oil biodiesel mixture. *Energy Convers. Manage.* **87**, 676–686 (2014).
- Elshaib, A. A., Kamal, M. M. & Elahwany, A. A. Performance of a diesel engine fueled by waste cooking oil biodiesel. *J. Energy Inst.* **87**, 11–17 (2014).
- Dai, X. *The Principle of Non-Ferrous Metallurgy*. Central South University Press, Changsha, 1998.
- Zhou, Y. Y. Copper slag depleted problem. *Nonferrous Min. Metall.* 50–52 (1988).
- Michal, E. J. & Schuhmann, R. Thermodynamics of iron-silicate slugs: slags saturated with solid silica. *Trans. Am. Inst. Min., Metall., Pet. Eng.* 723–728 (1952).
- Mafousek, J. Thermodynamics of iron oxidation in metallurgical slags. *JOM*. **64**, 1314–1320 (2012).
- Saito, N., Hori, N. & Nakashima, K. Viscosity of blast furnace slags. *Metall. Mater. Trans. B*. **34**, 509–516 (2003).
- Ji, F. Z. *et al.* Kinetics of coal injection into iron oxide containing slags. *Can. Metall. Q.* **44**, 85–94 (2005).
- Marin, T. & Utigard, T. Deoxidation of liquid copper with reducing O₂/CH₄ flames. *Metall. Mater. Trans. B*. **41**, 535–542 (2010).
- Warczok, A. & Utigard, T. A. Setting of copper drops in molten slags. *Metall. Mater. Trans. B* **26**, 1165–1173 (1995).
- Zhu, Z. Z. & Ma, K. Y. *Copper Metallurgy*. Yunnan Science and Technology Press, Kunming, 1995.
- Cardona, N. *et al.* Physical chemistry of copper smelting slags and copper losses at the Paipote smelter Part 1 – Thermodynamic modelling. *Can. Metall. Q.* **50**, 318–329 (2011).
- Zhou, G. F. & Xue, Z. L. *Iron and Steel Metallurgical Experiments*. Central South University Press, Changsha, 2008.
- Zhang, H. W. *et al.* Reduction of molten copper slags with mixed CO-CH₄-Ar gas. *Metall. Mater. Trans. B*. **45**, 582–589 (2014).
- Takeuchi, N. *et al.* Kinetic analysis of spherical wüstite reduction transported with CH₄ gas. *ISIJ Int.* **47**, 386–391 (2007).
- Nagasaka, T., Hino, M. & Ban-Ya, S. Interfacial kinetics of hydrogen with liquid slag containing iron oxide. *Metall. Mater. Trans. B*. **31**, 945–955 (2000).
- Utigard, T. *et al.* Reduction kinetics of liquid iron oxide-containing slags by carbon monoxide. *Metall. Mater. Trans. B*. **28**, 821–826 (1997).
- Huang, X. G. *Ferrous Metallurgy Principle*. Metallurgical Industry Press, Beijing, 2007.
- Toor, H. L. & Marchello, J. M. Film-penetration model for mass and heat transfer. *AIChE J.* **4**, 97–101 (1958).
- Hua, Y. X. *Introduction to dynamics of metallurgical processes*. Metallurgical Industry Press, Beijing, 2004.
- Meng, F. M. *Metallurgical Kinetic Foundation*. Metallurgical Industry Press, Beijing, 2014.
- Sasabe, M., Goto, S. K. & Someno, M. Rate of change of oxide chemical potential in liquid PbO-SiO₂ binary solution. *Metall. Mater. Trans. B*. **1**, 811–817 (1970).

Acknowledgements

Financial support for this study was supplied from the National Natural Science Foundation of China (No. U1602272 and 51664039), the Preliminary Research Program of the National Basic Research Program of China (No. 2014CB460605).

Author Contributions

B.L. and X.B.W. conceived and designed the experiments and performed the experiments; H.W., Y.G.W., and J.H.H. contributed reagents/materials/analysis tools. All authors contributed to the discussion of the results as well as to the writing of the manuscript. All authors read and approved the final manuscript.

Additional Information

Competing Interests: The authors declare that they have no competing interests.

Publisher's note: Springer Nature remains neutral with regard to jurisdictional claims in published maps and institutional affiliations.



Open Access This article is licensed under a Creative Commons Attribution 4.0 International License, which permits use, sharing, adaptation, distribution and reproduction in any medium or format, as long as you give appropriate credit to the original author(s) and the source, provide a link to the Creative Commons license, and indicate if changes were made. The images or other third party material in this article are included in the article's Creative Commons license, unless indicated otherwise in a credit line to the material. If material is not included in the article's Creative Commons license and your intended use is not permitted by statutory regulation or exceeds the permitted use, you will need to obtain permission directly from the copyright holder. To view a copy of this license, visit <http://creativecommons.org/licenses/by/4.0/>.

© The Author(s) 2017